Human Pathology (2019) **84**, 283–290

ELSEVIER

Human PATHOLOGY

www.elsevier.com/locate/humpath

Original contribution

Diagnosis of T-cell–mediated kidney rejection in formalin-fixed, paraffin-embedded tissues using RNA-Seq–based machine learning algorithms☆,☆☆

Peng Liu MS[a], George Tseng ScD[a], Zijie Wang MD[b], Yuchen Huang BS[b], Parmjeet Randhawa MD[b,*]

[a]*Department of Biostatistics, Graduate School of Public Health, University of Pittsburgh Medical Center, Pittsburgh, PA 15213, USA*

[b]*Department of Pathology, University of Pittsburgh Medical Center, Pittsburgh, PA 15213, USA*

Received 9 August 2018; revised 21 September 2018; accepted 29 September 2018

Keywords:
RNA-Seq;
Kidney;
Transplant;
Rejection;
Diagnosis;
Formalin;
Paraffin

Summary Molecular diagnosis is being increasingly used in transplant pathology to render more objective and quantitative determinations that also provide mechanistic and prognostic insights. This study performed RNA-Seq on biopsies from kidneys with stable function (STA) and biopsies with classical findings of T-cell–mediated rejection (TCMR). Machine learning tools were used to develop prediction models for distinguishing TCMR and STA samples using the top genes identified by DSeq2. The prediction models were tested on 703 biopsies with Affymetrix chip gene expression profiles available in the public domain. Linear discriminant analysis predicted TCMR in 55 of 67 biopsies labeled TCMR, and 65 of 105 biopsies designated as antibody-mediated rejection. The random forest and support vector machine models showed comparable performance. These data illustrate the feasibility of using RNA-Seq for molecular diagnosis of TCMR in formalin-fixed tissue. Application of the derived diagnostic algorithms to publicly available data sets demonstrates frequent coexistence of TCMR in biopsies designated as antibody-mediated rejection. This underrecognition of TCMR in renal allograft biopsies has significant implications with respect to patient care.

1. Introduction

Monitoring for T-cell–mediated rejection (TCMR) is an important element in the follow-up of kidney transplant recipients. Currently, an allograft biopsy is the commonest tool used for this purpose. Although it is an indispensable tool, the limitations of biopsy interpretation are well known. At this time, evaluation of biopsies is largely limited to morphologic analyses, which rely on subjective interpretations of lesions that are not highly specific. Diagnoses can be opinion based, and disease severity is communicated using ordinal scales that are prone to interobserver variation [1]. Reliable biopsy interpretation requires the availability of pathologists with significant experience, and such expertise is only available in tertiary medical centers.

Several studies are now available demonstrating the feasibility of using molecular technology for the tissue diagnosis of TCMR [2-5]. Typically, such studies use an additional core

☆ Competing interests: The authors have no conflicts of interest.
☆☆ Funding/Support: This research was supported by the Division of Transplantation Pathology, Department of Pathology, University of Pittsburgh.
* Corresponding author at: E737 UPMC-Montefiore Hospital, 3459 Fifth Ave, Pittsburgh, PA 15213.
E-mail address: randhawapa@upmc.edu (P. Randhawa).

https://doi.org/10.1016/j.humpath.2018.09.013
0046-8177/

of biopsy that is immediately processed and subjected to DNA microarray analysis to interrogate tissue gene expression. Comparisons of molecular and molecular diagnoses of TCMR have been associated with only a 28% to 77% agreement with histologic TCMR [6-8]. The superiority of the molecular over histologic analysis is often invoked in the discrepant cases, but sufficient consideration is not given to the fact that these 2 analyses are being performed on different cores of tissue, with the molecular core being substantially smaller. Indeed, one recent multicenter trial reports analyses of biopsies averaging as little as 3 mm in length [6]. Samples of this size do not meet the Banff criteria for tissue adequacy, and conclusions drawn from such samples need to be more closely examined. The long and successful use of histopathology in patient management suggests that the molecular result may not be the correct one in at least some of these discrepant cases, particularly those in which the diagnostic lesion is missing from the tissue subjected to molecular analysis. Commercial companies are now aggressively soliciting and performing molecular analyses on tissue fragments that may be too small to give robust results. Claims that such analyses are highly reproducible need to be taken with skepticism because the reproducibility data presented are derived from (*a*) allograft nephrectomy specimens where pathology is quite diffuse [9] or (*b*) needle biopsy data sets that did not contain sufficient numbers of biopsies with focally distributed pathology [10]. The focal distribution of lesions used to diagnose TCMR is well recognized, and this problem also occurs in about 20% to 30% of specimens, which is roughly the same as the prevalence of histology-microarray discrepancies.

One solution to formally investigate the effect of sampling on molecular diagnosis is to perform gene expression and histologic studies on the same core of biopsy tissue. This would require the ability to analyze formalin-fixed, paraffin-embedded (FFPE) tissue for transcriptomic profiles. Accordingly, this study seeks to evaluate the potential role of RNA-Seq as a means to establish a diagnosis of TCMR in routinely fixed biopsy tissue. RNA-Seq has notable advantages over DNA microarray technology in that it can interrogate more genes, with better quantitation and over a more extensive dynamic range, while allowing single-base resolution and detection of isoforms, microRNAs, and long-noncoding RNAs. The histologic severity and clinical course of TCMR vary among patients, and this may very well have a genetic and molecular basis, which can be further elucidated by RNA-Seq.

2. Materials and methods

2.1. Clinical material

This study was approved by the University of Pittsburgh's institution review board (protocol no. 10110393). The molecular signature discovery data set consisted of 5 kidney transplant patients with TCMR and 5 with stable renal function (STA). The age of these patients varied from 24 to 78 years, with a male-to-female ratio of 1.5: 1. All patients received thymoglobulin induction with a rapid 7-day corticosteroid taper. Dual-maintenance immunosuppressive therapy consisted of mycophenolate mofetil and tacrolimus. The time of biopsy varied from 95 to 380 days for patients with TCMR and 87 to 103 days for patients with STA. Assignment of histology diagnoses used criteria listed in the Banff 2015 schema of renal allograft pathology [11]. TCMR biopsies were graded as Banff 1A or 1B with no evidence of intimal arteritis. Biopsies from stable patients showed no significant pathologic change. The internal validation data set consisted of 10 additional TCMR biopsy samples from the departmental archives. The external validation data set consisted of 2 publicly available Gene Expression Omnibus (GEO) data sets [12,13] containing a total of 703 biopsies analyzed by Affymetrix Human Genome U133 Plus 2.0 Array (GSE48581 INTERCOM 300 Study and GSE36059 BFC403 study; Affymetrix, Santa Clara, CA).

2.2. RNA-Seq protocol

Biopsy tissue was minced into 1-mm^3 pieces and processed with the Invitrogen Pure Link FFPE tissue RNA Isolation kit for deparaffinization and total RNA extraction (Invitrogen, Carlsbad, CA). cDNA libraries were constructed from 100 ng total RNA obtained using the Ion Ampliseq Transcriptome Human Gene Expression Kit from Life Technologies (catalog

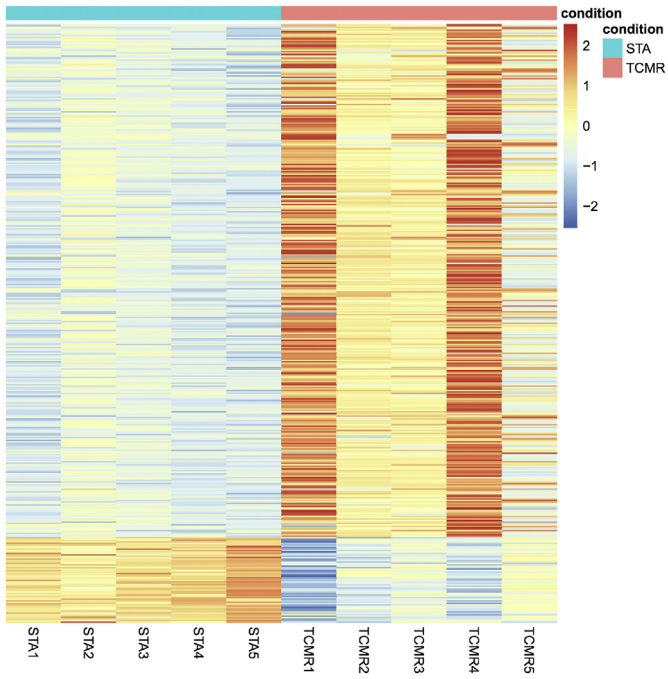

Fig. 1 Heat map of 421 DE genes in TCMR versus STA samples using the DESeq2 package. Rows depict expression of DE genes compared with STA values on an arbitrary scale, where STA expression is zero. Values greater than 0 and less than 0 represent up-regulation and down-regulation, respectively. Columns depict the samples designated as TCMR or STA using the color coding scheme indicated.

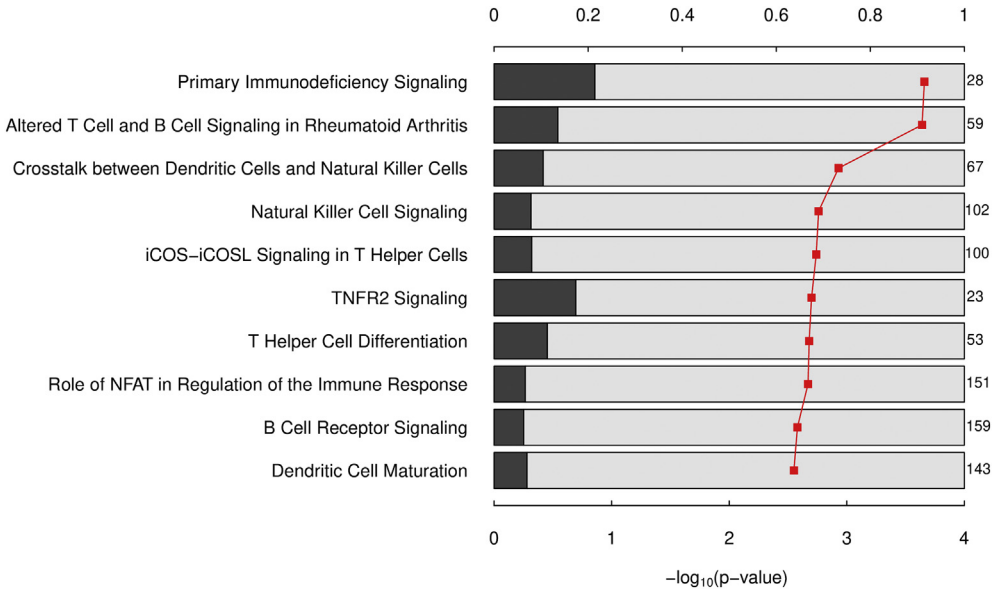

Fig. 2 Top 10 pathways associated with TCMR. The black and gray bars indicate the proportion of the DE genes and non-DE genes in each pathway. The total number of genes in each pathway is listed on the right side of the bar, and the $\log_{10} P$ values are plotted on the x-axis.

no. A26325; Carlsbad, CA) and the manufacturer's recommended protocol. Ampliseq Transcriptome analysis was performed by PrimBio Research Institute (Exton, PA) using an Ion Proton sequencer Ion Proton P1 chips, IonXpress barcodes, and Torrrent_Suite 5.0.4 software. cDNA libraries were constructed from 100 ng total RNA obtained using the Ion Ampliseq Transcriptome Human Gene Expression Kit from Life Technologies (catalog no. A26325) and the manufacturer's recommended protocol. The purified cDNA libraries were amplified by PCR using Library Amp Primers and run on Agilent 2100 Bioanalyzer to determine the yield and size distribution of each library. Approximately 100 pM of pooled barcoded libraries was used for templating using Life Technologies Ion Chef 200 kit (catalog no. 4488377).

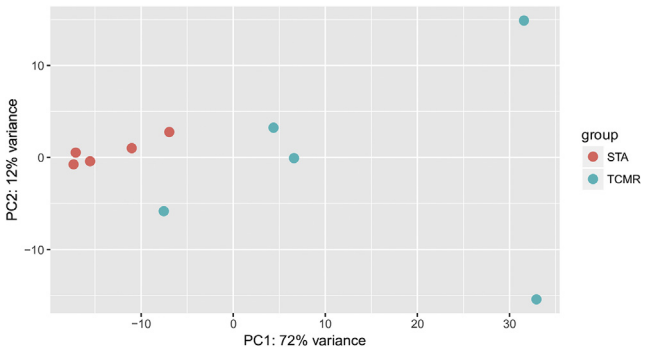

Fig. 3 Principal component analysis plot of the STA and TCMR samples using all 421 differentially expressed genes. The plot was generated using "plotPCA" function in "DESeq2" R package. The expression level of differentially expressed genes was normalized using "rlog" function in "DESeq2," which normalized the count data with respect to library size and transformed the data to the $\log_2$ scale.

2.2.1. Alignment and quality control

Raw sequence files (fastq) were aligned to the human transcriptome (hg19) reference sequences by the Strand NGS 3.0 (Strand Life Sciences, Bangalore, India) software using default parameters. The gene and transcript annotations used were retrieved from the Ensembl (https://4seast.ensembl.org) database. Aligned SAM files were used for further analysis. Quality control was assessed by the Strand NGS program, which determined the prealignment and postalignment quality of the reads for each sample. The aligned reads were then filtered, and reads that failed vendors QC were removed.

2.2.2. Differential expression and pathway analysis

For the RNA-Seq training data, differential expression (DE) analysis was implemented by an R package "DESeq2." (downloaded from https://bioconductor.org/packages/release/bioc/html) Transcripts with a mean count less than 5 were filtered out. A negative binomial generalized linear regression model was used to fit the RNA-Seq data, and Wald tests were performed to detect the significant differentially expressed genes based on 5 biologic replicates of each condition. For the microarray testing data, raw Affymetrix CEL files were downloaded from GEO and preprocessed using robust multichip averaging implemented in Bioconductor "affy" package. DE analysis was performed by an R package "limma": 54 675 probes were mapped to 23 003 Ensemble genes. When multiple probes were mapped to the same gene, the one with the largest interquartile range was chosen. For both RNA-Seq and microarray DE analyses, the resulting P values were adjusted by the Benjamini-Hochberg procedure for multiple comparisons. We set false discovery rate (FDR) threshold at 5%. All the above analyses were performed in R-3.4.3, an open source programming and software environment supported by the R Foundation for Statistical Computing, with various packages in Bioconductor 3.6. The Web-based tool

Table 1 Performance of an LDA-based classifier for the diagnosis of TCMR

Category in database	No. of cases designated as TCMR by classifier		
	INTERCOM data set	BFC data set	Combined data set
TCMR	87.5% (28/32)	77.1% (27/35)	82.1% (55/67)
ABMR	62.5% (25/40)	61.5% (40/65)	61.9% (65/105)
Mixed rejection	50.0% (3/6)	81.8% (18/22)	75% (21/28)
Total	71.8% (56/78)	69.7% (85/122)	70.5% (141/200)

Ingenuity Pathway Analysis was used for pathway analysis. Fisher exact test was used to test the association between TCMR and pathways.

2.3. Machine learning and validation

Three popular and interpretable machine learning methods were tested: linear discriminant analysis (LDA), support vector machines (SVM), and random forest (RF). LDA uses Gaussian assumptions and Bayes theorem to estimate the posterior probability of being classified as TCMR for each testing sample. Those with posterior probabilities greater than or equal to a specific cutoff are classified as TCMR. LDA was implemented by the "lda" function in the R package "MASS." The second method SVM separates the STA and TCMR samples by finding a higher-dimension hyperplane that maximizes the margin, which is the minimum distance of the objects to the hyperplane. SVM was implemented by the "svm" function in the R package "e1071." RF classifies the samples by a majority vote of random trees using the classification and regression tree algorithm. The trees are constructed by bootstrapping of samples and subsampling of features. This method was implemented using "randomForest" function in the R package "randomForest." For LDA and SVM, we selected the top N genes (N = 2-200) to construct the model. For LDA, we also tested 2 posterior probability cutoffs 0.1 and 0.2 for TCMR classification. The best combination of cutoff and N was selected from the highest Youden index by the performance in the testing sets. For RF, the method has embedded feature selection, so our input data are from all DE genes and there is no need to preselect N.

The prediction models were built by LDA, SVM, and RF methods using the RNA-Seq data. These models were then tested on 10 TCMR samples as internal validation and the publicly available data sets GSE48581 and GSE36059. We reported the model that yielded the largest Youden index (ie, sensitivity + specificity − 1).

3. Results

3.1. Quality control of RNA-Seq data

RNA purity assessed by the A260/A280 ratio ranged from 1.87 to 2.0. The RNA integrity numbers ranged from 2.0 to 2.5. RNA fragments of greater than 200 nucleotides in length comprised greater than 30% of the total RNA concentration. The mean sequence length in this RNA-Seq data set ranged from 66 to 117 nucleotides. After applying filters for low-quality reads, primer dimers, and polyclonal ion sphere particles, the number of usable reads derived from the Ion PI Chip/chips varied from 50% to 75%. This reflects the suboptimal quality of RNA in FFPE tissue. Greater than 98.5% of the reads aligned to the human transcriptome with accuracy rates of greater than 97%.

3.2. Alterations in gene expression and top pathways associated with TCMR

The number of transcripts in RNA-Seq data obtained from the STA and TCMR samples was 57 736, of which 19 864 remained after we excluded non–protein-coding RNA transcripts. We further filtered out the transcripts with a mean count of less than 5, after which 16 851 transcripts

Table 2 Performance of 3 machine learning algorithms for the diagnosis of TCMR

	Internal validation	INTERCOM study			BFC study		
	Sensitivity [a]	Sensitivity [a]	Specificity [a]	Youden index	Sensitivity [a]	Specificity [a]	Youden index
LDA	80.0% (8/10)	87.5% (28/32)	83.3% (5/6)	0.71	77.1% (27/35)	75.0% (6/8)	0.52
SVM	80.0% (8/10)	84.4% (27/32)	66.7% (4/6)	0.51	80.0% (28/35)	62.5% (5/8)	0.43
RF	90.0% (9/10)	87.5% (28/32)	100.0% (6/6)	0.88	74.3% (26/35)	75.0% (6/8)	0.49

[a] The sensitivity of each algorithm for the diagnosis of TCMR was dependent on the number of correct rejection calls in specimens known to have biopsy-proven rejection. The specificity was predicated on the number of "absence of rejection" calls in control nephrectomy specimens from nontransplanted kidneys, which by definition can never have a diagnosis of rejection. There are 6 control nephrectomies in the INTERCOM data set, and 5 of them were correctly predicted as TCMR negative. There are 8 nephrectomies in the BFC data set, and 6 of them were correctly predicted as TCMR negative. The incorrect predictions likely stem from inflammation and tissue injury secondary to (*a*) surgical manipulation and (*b*) the underlying disease for which the nephrectomy procedure was performed.

were left. We identified a total number of 421 DE genes at 5% FDR threshold (Fig. 1), of which 361 were up-regulated and 60 were down-regulated. Fold changes greater than 2-fold change (FC), greater than 5 FC, and greater than 10 FC were respectively seen in 420, 256, and 63 transcripts; 385 of 412 DE genes of training data matched corresponding probes in testing data sets. As a validation, among the 385 DE genes of training data, 207 and 152 of the genes, respectively, were also DE genes in testing GEO data sets (GSE48581 and GSE36059) under 5% FDR. This indicates the substantial consistency of DE genes between the RNA-Seq and microarray data sets. The DE analysis result was further used to identify the pathways associated with TCMR. The top 10 pathways are listed in Fig. 2. After Benjamini-Hochberg correction, the primary immunodeficiency signaling pathway and altered T cell and B cell signaling in the rheumatoid arthritis pathway were significantly altered (FDR <0.05).

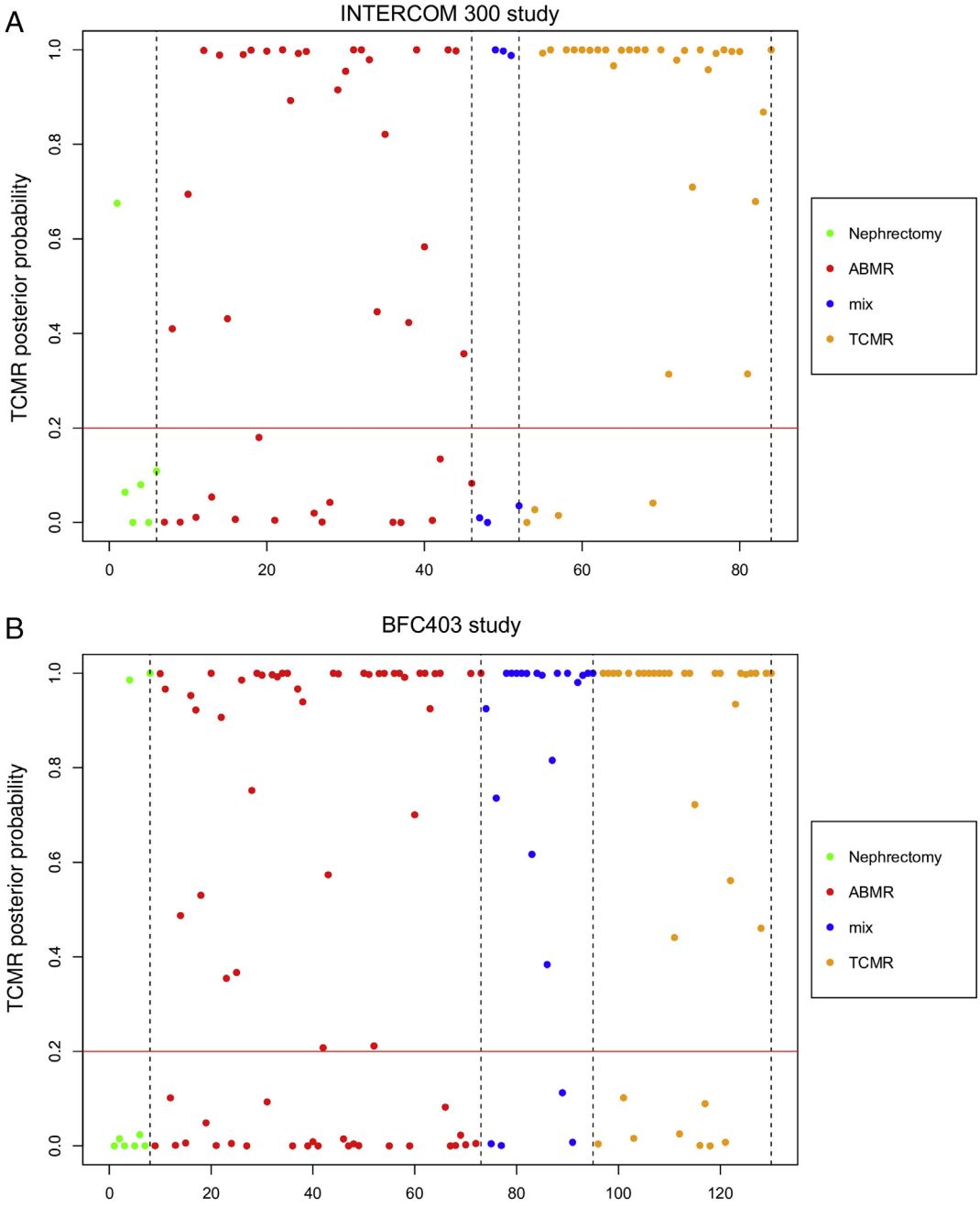

Fig. 4 The posterior probability of samples classified as TCMR using LDA method in the INTERCOM 300 study (A) and BFC403 study (B). The samples are represented by their diagnosis: nephrectomy (green dots), AMBR (red dots), mixed (blue dots), and TCMR (orange dots). Nephrectomy means healthy kidney tissue around tumor tissue removed by surgery. The horizontal line 0.2 is the cutoff. Samples with a posterior probability of greater than 0.2 are classified as TCMR.

3.3. Development and validation of a RNA-Seq–based molecular classifier

As a proof of concept, principal component analysis using all DE genes showed separate clustering of STA and TCMR samples (Fig. 3). We used the 421 identified DE genes and applied the LDA, RF, and SVMs algorithms to construct classifiers using TCMR and STA biopsies as the training data set. The classifiers were then applied to an internal validation data set of 10 additional TCMR biopsies and 2 external validation data sets comprising the INTERCOM 300 and BFC403 data sets. For LDA, a combination of the top 33 genes with a 0.2 cutoff was chosen to achieve the highest Youden index. Increasing the number of genes included in the model from 33 to 200 did not substantially improve test performance (Supplementary Fig. S1). It was observed that LDA and RF methods had superior performance to SVM (Tables 1 and 2). Using the LDA method, the prediction model achieved correctly

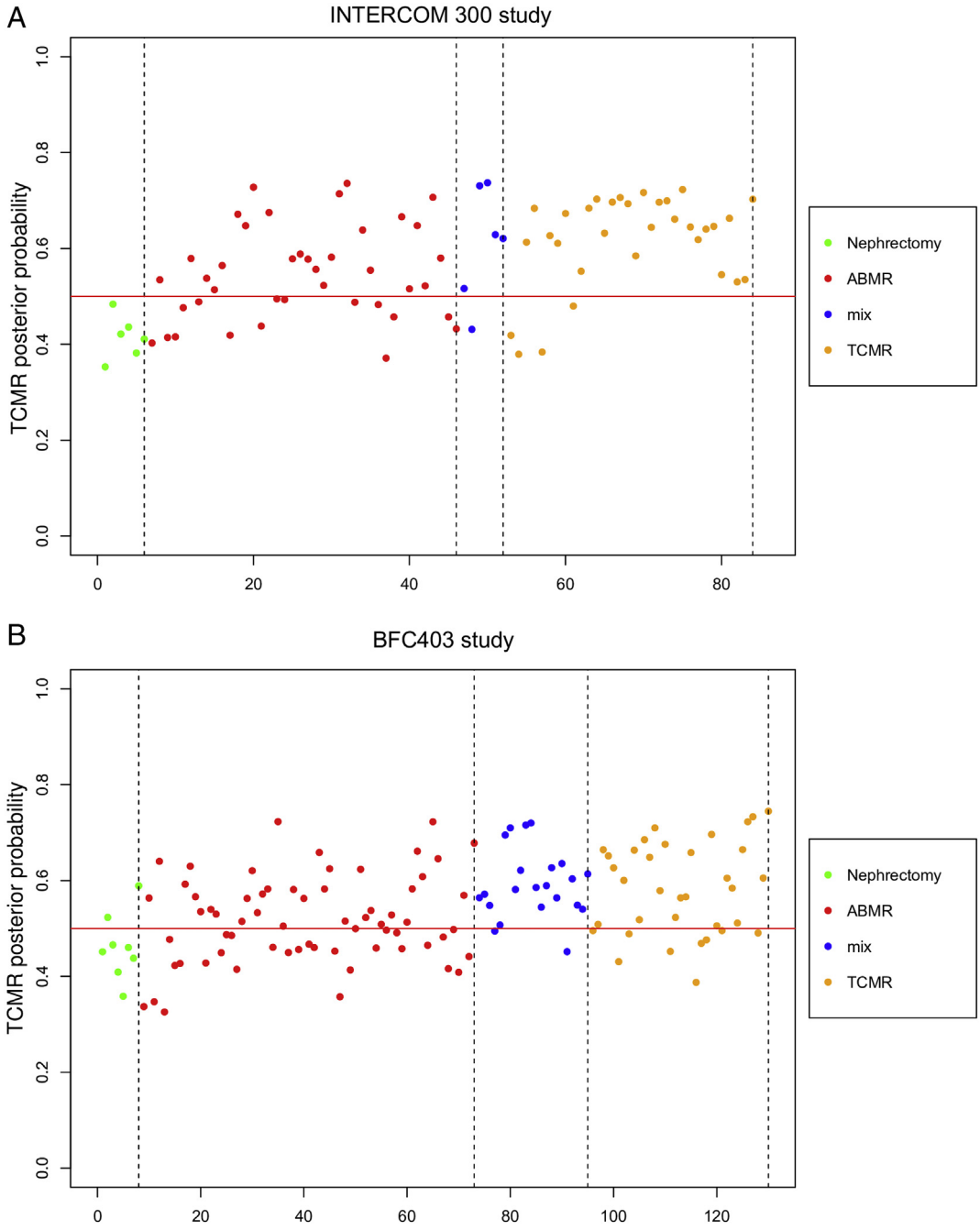

Fig. 5 The fraction of the "votes" for TCMR from RF method in the INTERCOM 300 Study (A) and BFC403 study (B). The samples are represented by their diagnosis: nephrectomy (green dots), AMBR (red dots), mixed (blue dots), and TCMR (orange dots). Nephrectomy specimens represent normal tissue around surgically resected renal cell carcinomas. The horizontal line 0.5 separates the samples with and without TCMR.

identified 8 of 10 TCMR samples in internal validation. The model also achieved 88% sensitivity (28/32) and 83% specificity (5/6) in the INTERCOM 300 Study and 77% sensitivity (27/35) and 75% specificity (6/8) in the BFC403 study (Table 2 and Fig. 4). Meanwhile, the RF method correctly identified 9 of 10 TCMR samples in internal validation, and at the same time, it achieved 88% sensitivity (28/32) and 100% specificity (6/6) in the INTERCOM 300 Study and 74% sensitivity (26/35) and 75% specificity (6/8) in the BFC403 study (Fig. 5). In addition, using the LDA method, TCMR was identified in 25 (62.5%) of 40 and 40 (61.5%) of 65 biopsies designated as antibody-mediated rejection (ABMR) in the INTERCOM 300 Study and BFC403 study, respectively. If mixed TCMR-ABMR samples were included in the TCMR category, the sensitivities were 81.5% (31 of 38) and 78.9% (45 of 57) for the INTERCOM 300 Study and BFC403 study, respectively. Combining both the external validation data sets LDA predicted TCMR in 55 (82.1%) of 67 biopsies labeled TCMR, 65 (61.9%) of 105 biopsies designated as ABMR, and 21 (75.0%) of 28 biopsies classified as mixed rejection. Similar findings were observed using the RF method.

4. Discussion

The goal of this study was to develop an RNA-Seq–based method for the diagnosis of TCMR in FFPE tissue. The primary impetus behind this effort was to allow both the histologic and the molecular evaluations to be performed on the same biopsy core. This would facilitate better assessment of the potential contribution of sampling error to discrepancies between histologic and molecular diagnoses. The dependence of histologic assessment on sample size is well known. In 2 independent studies, examination of 2 cores of biopsy tissue instead of a single core led to a significant difference in diagnosis in ~10% of samples [14,15]. An even more striking effect has been reported in patients with polyomavirus BK nephropathy, wherein viral infection could be demonstrated in both available cores of tissue in only 37.5% of biopsies [16]. One would expect that if histologic lesions are subject to sampling considerations, there would be corresponding differences in the molecular profiles. Molecules can certainly diffuse beyond the actual lesions, but the fall in concentration would significantly alter the diagnostic performance of the molecular classifiers. Recently, Madill-Thomsen et al [10] showed comparable gene expression profiles in 26 paired cortical and medullary samples obtained from the same biopsy core. However, more than half of these biopsies were in categories designated “normal, no major abnormalities, or acute kidney injury,” and one would not expect much regional variation of pathology in this setting. There was an insufficient representation of biopsies with TCMR (n = 2) or borderline change (n = 2) where the uneven distribution of lesions is a significant problem in approximately 20% to 30% of all biopsies. Importantly, these replicate cores were only 1 to 3 mm long and not well suited to study a problem that can only be appreciated on longer cores of tissue. Larger studies directly comparing histologic and molecular diagnosis obtained from the same tissue fragments are needed, and the ability to perform both analyses on FFPE tissues should facilitate this effort.

Performing gene expression on FFPE is known to be challenging [17,18]. RNA integrity, mean sequence length, percent of usable reads, and alignment statistics for our samples were all lower than what is typical of frozen tissue. However, the high-throughput nature of RNA-Seq allowed us to obtain a sufficient number of quality reads for diagnostically useful information to be obtained. The DESeq2 package identified 421 transcripts differentially expressed between the STA and TCMR patient groups: 207 and 152 of these genes were differentially expressed in data sets GSE348581 and GSE36059 derived from fresh-frozen TCMR tissue. Moreover, the LDA algorithm derived from our RNA-Seq data was able to confirm a diagnosis of TCMR in most of these samples that had been previously assigned to this category using a different assay platform (Affymetrix gene chips). Thus, our data clearly demonstrate the feasibility of obtaining meaningful RNA-Seq signatures from FFPE tissues.

It is notable that samples categorized as ABMR in publicly available data sets frequently satisfied our RNA-Seq–based criteria for TCMR. This illustrates the important point that TCMR and ABMR are not mutually exclusive diagnoses. It is likely that many biopsies that get labeled simply as ABMR have concurrent TCMR. Indeed, when formally studied, the reported incidence of mixed TCMR-ABMR varies from 6% to 48% in different studies and can be as high as 96% if late biopsies with ABMR and borderline T-cell infiltrates considered [19-21]. It is sometimes argued that T-cell infiltration and tubulitis in these cases are a secondary phenomenon. This may very well be true in some cases, but in other patients, TCMR can be shown to precede ABMR. The relative frequency with which these 2 scenarios play out is difficult to determine in the clinical setting because biopsies appropriately timed to answer this question are usually not available. In one recent study, de novo donor-specific antibody had a 25% specificity for the diagnosis of TCMR [22]. In a nonhuman primate model, TCMR preceded ABMR in more than one-half of kidney recipients [23]. Molecular studies show a significant overlap in gene expression profiles of biopsies with ABMR and TCMR, and the burden of cytotoxic T lymphocyte–associated transcripts is also comparable [9,24]. RNA-Seq–based classifiers for ABMR have not yet been reported.

The principal limitation of this study is the small number of samples analyzed by RNA-Seq. However, this shortcoming has been counterbalanced by supplementary analyses of 703 biopsies available in the public domain. Another potential caveat is that RNA-Seq results have not been validated by quantitative PCR. This does not seem necessary because many of the TCMR-associated genes found to be differentially expressed by RNA-Seq analysis overlap with prior studies that used DNA microarray technology. The same observation was made previously in biopsies with polyomavirus BK nephropathy,

wherein virus-associated changes in gene expression showed comparable fold change and similar *P* values irrespective of which technology was used to obtain the data [25]. Another recent study that performed DNA microarray analysis and RNA-Seq in parallel on the same specimens has noted that gene expression profiling is platform agnostic [26].

In conclusion, this study establishes RNA-Seq as a tool that is quite suitable for molecular diagnosis of TCMR in FFPE tissues. It adds to mounting evidence that many biopsies simply labeled as ABMR are, in fact, examples of mixed T cell and ABMR. This has obvious ramifications for the proper management of these patients. Additional work is needed to develop molecular signatures for other important biopsy categories such as pyelonephritis, drug hypersensitivity reactions, autoimmune disorders, paraprotein related pathology, and recurrent glomerulonephritis. All these diseases have mononuclear cell infiltrates that may share gene expression patterns of T-cell activation in common with TCMR. The possibility that this may lead to false-positive molecular diagnoses of TCMR deserves more systematic study. The inability to distinguish TCMR from BKV nephropathy purely by transcriptomics data has been noted [25].

Supplementary data

Supplementary data to this article can be found online at https://doi.org/10.1016/j.humpath.2018.09.013.

References

[1] Furness PN, Taub N, Assmann KJ, et al. International variation in histologic grading is large, and persistent feedback does not improve reproducibility. Am J Surg Pathol 2003;27:805-10.

[2] Reeve J, Sellares J, Mengel M, et al. Molecular diagnosis of T cell-mediated rejection in human kidney transplant biopsies. Am J Transplant 2013;13:645-55.

[3] Modena BD, Kurian SM, Gaber LW, et al. Gene expression in biopsies of acute rejection and interstitial fibrosis/tubular atrophy reveals highly shared mechanisms that correlate with worse long-term outcomes. Am J Transplant 2016;16:1982-98.

[4] Sigdel TK, Bestard O, Salomonis N, et al. Intragraft antiviral-specific gene expression as a distinctive transcriptional signature for studies in polyomavirus-associated nephropathy. Transplantation 2016;100:2062-70.

[5] Maluf DG, Dumur CI, Suh JL, et al. Evaluation of molecular profiles in calcineurin inhibitor toxicity post–kidney transplant: input to chronic allograft dysfunction. Am J Transplant 2014;14:1152-63.

[6] Halloran PF, Reeve J, Akalin E, et al. Real time central assessment of kidney transplant indication biopsies by microarrays: the INTERCOMEX study. Am J Transplant 2017;17:2851-62.

[7] de Freitas DG, Sellares J, Mengel M, et al. The nature of biopsies with "borderline rejection" and prospects for eliminating this category. Am J Transplant 2012;12:191-201.

[8] Halloran PF, Famulski KS, Reeve J. Molecular assessment of disease states in kidney transplant biopsy samples. Nat Rev Nephrol 2016;12:534-48.

[9] Mueller TF, Einecke G, Reeve J, et al. Microarray analysis of rejection in human kidney transplants using pathogenesis-based transcript sets. Am J Transplant 2007;7:2712-22.

[10] Madill-Thomsen KS, Wiggins RC, Eskandary F, Bohmig GA, Halloran PF. The effect of cortex/medulla proportions on molecular diagnoses in kidney transplant biopsies: rejection and injury can be assessed in medulla. Am J Transplant 2017;17:2117-28.

[11] Loupy A, Haas M, Solez K, et al. The Banff 2015 kidney meeting report: current challenges in rejection classification and prospects for adopting molecular pathology. Am J Transplant 2017;17:28-41.

[12] Halloran PF, Pereira AB, Chang J, et al. Potential impact of microarray diagnosis of T cell-mediated rejection in kidney transplants: the INTERCOM study. Am J Transplant 2013;13:2352-63.

[13] Sellares J, Reeve J, Loupy A, et al. Molecular diagnosis of antibody-mediated rejection in human kidney transplants. Am J Transplant 2013;13:971-83.

[14] Sorof JM, Vartanian RK, Olson JL, Tomlanovich SJ, Vincenti FG, Amend WJ. Histopathological concordance of paired renal allograft biopsy cores. Effect on the diagnosis and management of acute rejection. Transplantation 1995;60:1215-9.

[15] Colvin RB, Cohen AH, Saiontz C, et al. Evaluation of pathologic criteria for acute renal allograft rejection: reproducibility, sensitivity, and clinical correlation. J Am Soc Nephrol 1997;8:1930-41.

[16] Drachenberg CB, Papadimitriou JC, Hirsch HH, et al. Histological patterns of polyomavirus nephropathy: correlation with graft outcome and viral load. Am J Transplant 2004;4:2082-92.

[17] Bass BP, Engel KB, Greytak SR, Moore HM. A review of preanalytical factors affecting molecular, protein, and morphological analysis of formalin-fixed, paraffin-embedded (FFPE) tissue: how well do you know your FFPE specimen? Arch Pathol Lab Med 2014;138:1520-30.

[18] Kojima K, April C, Canasto-Chibuque C, et al. Transcriptome profiling of archived sectioned formalin-fixed paraffin-embedded (AS-FFPE) tissue for disease classification. PLoS One 2014;9:e86961.

[19] Sellares J, de Freitas DG, Mengel M, et al. Understanding the causes of kidney transplant failure: the dominant role of antibody-mediated rejection and nonadherence. Am J Transplant 2012;12:388-99.

[20] El-Zoghby ZM, Stegall MD, Lager DJ, et al. Identifying specific causes of kidney allograft loss. Am J Transplant 2009;9:527-35.

[21] Dorje C, Midtvedt K, Holdaas H, et al. Early versus late acute antibody-mediated rejection in renal transplant recipients. Transplantation 2013;96:79-84.

[22] Wiebe C, Gareau AJ, Pochinco D, et al. Evaluation of C1q status and titer of de novo donor-specific antibodies as predictors of allograft survival. Am J Transplant 2017;17:703-11.

[23] Adam BA, Smith RN, Rosales IA, et al. Chronic antibody-mediated rejection in nonhuman primate renal allografts: validation of human histological and molecular phenotypes. Am J Transplant 2017;17:2841-50.

[24] Adam B, Afzali B, Dominy KM, et al. Multiplexed color-coded probe-based gene expression assessment for clinical molecular diagnostics in formalin-fixed paraffin-embedded human renal allograft tissue. Clin Transplant 2016;30:295-305.

[25] Pan L, Lyu Z, Adam B, et al. Polyomavirus BK nephropathy–associated transcriptomic signatures: a critical reevaluation. Transplant Direct 2018;4:e339.

[26] Kurian SM, Velazquez E, Thompson R, et al. Orthogonal comparison of molecular signatures of kidney transplants with subclinical and clinical acute rejection: equivalent performance is agnostic to both technology and platform. Am J Transplant 2017;17:2103-16.